Tris(1,2-ethanediamine) complexes of osmium(IV), osmium(III) and osmium(II): oxidative dehydrogenation reactions

Peter A. Lay*
Department of Inorganic Chemistry, The University of Sydney, Sydney, NSW 2006 (Australia)
and Alan M. Sargeson*
Research School of Chemistry, Australian National University, G.P.O. Box 4, Canberra, ACT 2601 (Australia)

Abstract

The reaction of $[NH_4]_2[OsBr_6]$ with neat 1,2-ethanediamine (en) yields *cis*-$[Os(en\text{-}H)_2(en)]Br_2$, which is recrystallized as *cis*-$[Os(en\text{-}H)_2(en)]I \cdot Br$ in 40–50% yield. $[Os(en)_3]Br_3 \cdot 2H_2O$ is obtained from the filtrate in ~40% yield by the addition of EtOH, to give a recovery of ~90% of osmium 1,2-ethanediamine complexes. This *cis*-$[Os(en\text{-}H)_2(en)]^{2+}$ complex protonates to form $[Os(en\text{-}H)(en)_2]^{3+}$ and both Os^{IV} complexes have been characterized by ^1H and ^{13}C NMR, IR and UV–Vis spectroscopies. Since the N–H exchange rate for the doubly deprotonated Os^{IV} complex is slow at the amido sites their *cis* relationship is maintained. The Os^{IV} complexes are reduced readily to $[Os(en)_3]^{3+}$ by a variety of reductants. A reversible $Os^{III/II}$ couple is observed at −0.52 V versus NHE in 0.1 M $NaCF_3SO_3$. All of these complexes are oxidized in air to form $[Os(en)_2(diim)]^{2+}$ (diim = ethanediimine) and $[Os(en)(diim)_2]^{2+}$ as the eventual product. The latter were characterized by ^1H and ^{13}C NMR, UV–Vis and IR spectroscopy. The mechanism of the dehydrogenation reaction is discussed in detail, in relation to related Fe and Ru amine chemistry.

Introduction

The preparations of *cis*-$[Os(en)(en\text{-}H)_2]Br_2$, $[Os(en)_2(en\text{-}H)]Br_3$ and $[Os(en)_3]^{3+}$ were first reported by Dwyer and Hogarth in the 1950s [1, 2]. However, at the time when this chemistry was reexamined [3], it was not clear whether the Os^{IV} complexes had been correctly formulated, since the equivalent putative Ru^{IV} analogue, $[Ru(en\text{-}H)_2(en)]^{2+}$ [4], was later shown to be $[Ru(en)_2(diim)]^{2+}$ [5]. We have reported preliminary results on the chemistry and X-ray crystallographic analyses of *cis*-$[Os^{IV}(en)(en\text{-}H)_2]Br_2$ [6] and $[Os^{III}(en)_3](CF_3SO_3)_3 \cdot H_2O$ [7] which established that the original formulations of Dwyer and Hogarth [1, 2] were correct. Here, details of this chemistry and the implications for the mechanisms of oxidative dehydrogenation reactions are reported. Particularly pertinent to this understanding are recent development in analogous tmen chemistry (tmen = 2,3-dimethyl-2,3-butanediamine) [8] and the oxidative dehydrogenation of complexes of Ru [9, 10].

*Authors to whom correspondence should be addressed.

Experimental

Absorption spectra and molar absorptivities (ϵ, M^{-1} cm^{-1}) were recorded by using Cary 14 and 118C spectrophotometers. ^1H NMR spectra were recorded with a JEOL 60 and 100-MHz Minimar spectrometers using sodium 3-(trimethylsilyl)propanesulfonate (NaTPS) or tetramethylsilane (TMS) as internal standards. ^1H-decoupled ^{13}C NMR spectra were obtained by using a JNM-FX 60 Fourier transform spectrometer (15.09 MHz) with 1,4-dioxane as an internal standard. All chemical shifts (δ) are expressed in ppm as positive, downfield shifts relative to these standards. IR spectra were recorded from KBr disks on a Perkin-Elmer 457 or 683 IR spectrometer. Magnetic susceptibility measurements were performed using the Gouy method and a Newport Instruments Electromagnet Type C in conjunction with a Stanton Instruments SM 12/S Balance. The field was calibrated with $Hg[Co(SCN)_4]$. ESR spectra were obtained from a JEOL JES-PE ESR spectrometer using diphenyl picryl hydrazyl (DPPH) as calibrant.

Standard electrochemical measurements were performed with either a PAR model 174A polarographic analyzer coupled with a Houston Instruments Omi-

0020-1693/92/$5.00

nographic 2000 recorder or a PAR model 170 electrochemistry system. Coulometric measurements were achieved with a PAR model 173 potentiostat–galvanostat containing a model 179 digital coulometer insert or an Amel model 731 digital integrator in conjunction with an Amel model 551 potentiostat. PAR coulometry cell systems, models 9800 or 377A, or coulometry cells of our own design, were used in such measurements, with a mercury pool or platinum basket as working electrode.

In all experiments, the conventional three-electrode system was used with positive feedback *IR* compensation in voltammetric experiments. The auxiliary electrode was platinum wire (or gauze, for coulometry), and the reference electrode was saturated calomel (SCE) or Ag/AgCl/LiCl (saturated in acetone) for aqueous or non-aqueous solutions, respectively. A salt bridge containing the solvent and electrolyte used in the working compartment separated the reference electrode from the solution in that compartment. For voltammetry, the working electrode was a PAR model 172A dropping mercury electrode (DME), platinum or gold wire, or a Beckmann rotating Pt disk. Certain experiments were performed with a PAR model 303 static dropping mercury electrode (SMDE) interfaced with the PAR model 170 with a Ag/AgCl/saturated KCl reference electrode (water); this electrode has the capacity to operate as a hanging mercury drop electrode (HMDE). All solutions were degassed with N_2 or Ar that had been presaturated with the solvent used in the working compartment of the cell.

Ion exchange resins, SP-Sephadex C-25 and Dowex 50W-X2 (Bio-Rad 200–400 mesh), were used for separation of the complexes and desalting, respectively. All column dimensions are given as length by diameter in centimeters. Evaporations were performed at reduced pressure (~20 torr) with a Büchi rotary evaporator and a bath at 50 °C. Distilled water, acetone (Univar AR or Proanalys AR) and acetonitrile (Riedel-De Haën, AG or Univar AR) were used without further purification. $NaCF_3SO_3$ and CF_3SO_3H were used as supporting electrolytes in water, while $R_4NCF_3SO_3$ salts [11] were used in non-aqueous solvents.

All microanalyses were performed by the Australian National University Microanalytical Service. It was often necessary to perform a Kirsten–Dumas analysis for N in order to obtain satisfactory microanalyses for this element [6].

OsO_4 ampoules (Johnson Matthey Chemicals) were used to prepare $(NH_4)_2[OsBr_6]$ by the standard method [12]. $[Os(NH_3)_6]I_3$ was obtained by a modification [13] of the method of Hogarth and Dwyer [14].

Preparations and manipulations requiring an inert atmosphere were performed under an N_2 blanket in a glove bag or a Lintott Engineering glove box.

$[Os(en\text{-}H)_2(en)]X_2$ (X=I, Br) and $[Os(en)_3]Br_3 \cdot 3H_2O$

These were obtained from the reaction of $(NH_4)_2[OsBr_6]$ using a modification of the method of Dwyer and Hogarth [2]. The reaction was performed as described previously, except dry 1,2-ethanediamine was used and the reaction and manipulations were performed under N_2. The bromide salt so obtained was recrystallized in poor yield by evaporation of a H_2O:EtOH:Et_2O solution (1:10:2) of the complex under a stream of N_2. *Anal.* Calc. for $OsC_6H_{22}N_6Br_2$: C, 13.69; H, 3.83; N, 15.97; Br, 30.4. Found: C, 13.7; H, 4.3; N, 16.0; Br, 29.3%. ^1H NMR (D_2O, pH 7): 2.7br multiplet, CH_2; ^{13}C NMR (D_2O, pH 7) −23.8. This procedure gave crystals suitable for an X-ray crystal structure analysis [6].

The crude bromide from the reaction mixture was more conveniently purified in high yield by precipitation of the mixed I–Br salt. To a deaerated solution of the crude bromide dissolved in the minimum of water at ~20 °C, was added an equal volume of deaerated saturated NaI solution. The solution was cooled in ice under a N_2 atmosphere; the crystals were collected, washed with acetone and diethyl ether and dried *in vacuo* over P_4O_{10}. *Anal.* Calc. for $OsC_6H_{22}N_6IBr$: C, 12.53; H, 3.85; N, 14.61; Br, 13.89. Found: C, 12.3; H, 3.8; N, 14.8; Br, 13.9%. UV–Vis (pH 8.5; Tris/HCl): 223 (40,000), 270sh, 550 (20). The yield of the mixed I^-/Br^- salt is 40–50% based on $(NH_4)_2[OsBr_6]$.

The filtrate from the initial reaction mixture was treated with deaerated EtOH (ten-fold excess) producing a grey-brown precipitate, which was rapidly filtered. The hygroscopic solid was recrystallized from aqueous HBr in the manner described by Dwyer and Hogarth for $[Os(en\text{-}H)(en)_2]Br_3 \cdot 3H_2O$ [2]. However the olive-green precipitate was shown by microanalysis, IR and magnetic measurements (μ_{eff}=1.6 BM) to be $[Os(en)_3]Br_3 \cdot 0.5HBr\text{–}2H_2O$. *Anal.* Calc. for $C_6H_{28.5}N_6O_2Br_{3.5}Os$: C, 11.15; H, 4.37; N, 13.01; Br, 37.1. Found: C, 11.3; H, 4.6; N, 12.5; Br, 38.5%. The yield of the Os^{III} complex was ~40% giving an overall yield of Os/1,2-ethanediamine complexes of 80–90% based on $(NH_4)_2[OsBr_6]$.

$[Os(en\text{-}H)(en)_2]Br_3 \cdot 3H_2O$

This was obtained as bright green needle-like crystals by treatment of crude pink $[Os(en\text{-}H)_2(en)]Br_2$ with aqueous HBr [2]. *Anal.* Calc. for $C_6H_{29}N_6O_3Br_3Os$: C, 10.86; H, 4.41; N, 12.68; Br, 36.2. Found: C, 10.9; H, 4.7; N, 12.5; Br, 38.8%. ^1H NMR (0.1 M DCl, 60 MHz): 2.7br, multiplet, CH_2, ^{13}C NMR (0.1 M DCl): −29.9.

[Os(en-H)(en)$_2$]ZnBr$_4$·Br·H$_2$O

This was obtained as green needles by treatment of a warm solution (50 °C) of [Os(en-H)(en)$_2$]Br$_3$·3H$_2$O with saturated Li$_2$ZnBr$_4$ solution and allowing to cool. *Anal.* Calc. for $C_6H_{25}N_6OBr_5Zn$: C, 8.49; H, 3.07; Zn, 7.7. Found: C, 8.6; H, 3.2; Zn, 8.2%.

Crystals of both of these salts were examined by X-ray crystallography but were found to be twinned [15].

[Os(en)$_3$]I$_3$·2H$_2$O

This was prepared from crude *cis*-[Os(en-H)$_2$(en)]Br$_2$ by reduction with $Na_2S_2O_4$ [2] to yield a yellow powder.

[Os(en)$_3$]Cl$_3$·3H$_2$O

This was obtained from the bromide salt in the following manner. The bromide salt was dissolved in the minimum amount of warm aqueous (90%) ethanol (40 °C) and HCl (36%) added dropwise until cloudiness occurred. The solution was heated until the turbidity disappeared and on cooling slowly to room temperature and then to 6 °C, colorless needles were formed. Again, twinning problems precluded an X-ray crystallographic analysis of this and the bromide salt [15].

[Os(en)$_3$](CF$_3$SO$_3$)$_3$ and [Os(en)$_3$](CF$_3$SO$_3$)$_3$·H$_2$O

A solution of [Os(en)$_3$]Br$_3$ (0.5 g) in distilled CF_3SO_3H (5 ml) was heated at 90 °C for 10 min to liberate HBr gas. After cooling to 0 °C, diethyl ether (50 ml) was added dropwise with constant stirring. **Caution**: This is a very exothermic process. The fine white powder was collected and washed thoroughly with diethyl ether to give a quantitative yield of the anhydrous salt. *Anal.* Calc. for $C_9H_{24}F_9N_6O_9S_3Os$: C, 13.22; H, 2.96; N, 10.28; S, 11.76; F, 20.91. Found: C, 13.2; H, 3.3; N, 9.9; S, 11.7; F, 21.2%. Colorless block-like crystals of the hydrate, [Os(en)$_3$](CF$_3$SO$_3$)$_3$·H$_2$O, that were used for the X-ray structure determination [7], were obtained by slow crystallization of the triflate salt from a 50% aqueous CF_3SO_3H solution maintained at 0 °C.

[Os(en)(diim)$_2$]Cl·HCl·H$_2$O

A solution of the crude *cis*-[Os(en)(en-H)$_2$]Br$_2$ (0.5 g) in water (10 ml) was allowed to stand exposed to air at 20 °C for 3 weeks. After filtration, the solution was diluted to 500 ml and sorbed on a column of SP-Sephadex C-25 (3 cm wide, 20 cm diam.). The column was washed with water (500 ml) and eluted with 0.1 M NaCl to yield a minor pale green band. Upon elution with 0.2 M NaCl, a minor brown band preceeded an intensely coloured dark brown band. The first two bands only contained a few milligrams of complex each which were not characterized. The major band was sorbed on a column of Dowex 50W-X2 (2 cm wide, 3 cm diam.) and after washing the column with water (500 ml) and 0.5 M HCl (500 ml), was eluted with 2 M HCl. Evaporation of the eluant until almost all the solvent was removed, followed by the careful addition of acetone (15 ml) gave a black–brown precipitate which was collected, washed with diethyl ether, and dried *in vacuo* over P_2O_5. Yield (0.2 g, 43%). *Anal.* Calc. for $C_6H_{19}Cl_3N_6OOs$: C, 14.77; H, 3.93; Cl, 21.8. Found: C, 14.7; H, 3.7; Cl, 23.1%. ^{1}H NMR (D_2O): 2.61 (br, 2, CH_2); 2.93 (br, 2, CH_2); ~4.8 (br, NH_2, obscured by HDO peak); 6.41 (br, 2, NH_2); 8.51, 8.58 (AB quartet, 2 C*H*=NH); 11.65 (br, 2, –CH=NH); 14.07 (br, 2, CH=N*H*). ^{13}C NMR (D_2O): +102.8 (*trans*-CH=NH); +97.7 (*cis*-CH=NH); −18.6 (en). IR (KBr): ν(CH=NH) 1478 and 1483 cm^{-1}; Vis–UV (H_2O): 380 (4.5×10^3) sh; 423 (14.1×10^3) 500 ($6.\times10^3$) sh; 653 (75). During the elution procedure, black residues remained at the tops of the columns which reduced the yields. However this problem was minimized by doing the separations rapidly.

The chloride salt was recrystallized by the addition of a saturated $LiZnCl_4$ solution to an aqueous solution of the chloride salt. At the onset of turbidity, the solution was heated on a steam bath, then cooled slowly to 20 °C. Further cooling overnight in a refrigerator yielded black block-like crystals of [Os(en)-(diim)$_2$]ZnCl$_4$, however, attempts to solve the structure have not been successful [15].

Solid-state reactivity of cis-[Os(en)(en-H)$_2$]Br$_2$

A solid sample of *cis*-[Os(en)(en-H)$_2$]Br$_2$ (0.5 g) was exposed to air for four months. The solid was dissolved in water, 500 ml, and sorbed on a column of SP-Sephadex C-25. Rapid elution with 0.2 M NaCl produced a faster moving yellow–green band, which overlapped an intensely brown band. The combined band of 2+ ions was evaporated to dryness, redissolved and the visible spectrum measured.

Reactivity of cis-[Os(en)(en-H)$_2$]$^{2+}$

The decay of an oxygen free solution of *cis*-[Os(en)(en-H)$_2$]Br$_2$ was monitored at pH 7.0 (NaH_2PO_4/Na_2HPO_4 0.01 M)* with the ionic strength adjusted to 0.20 M ($NaCF_3SO_3$). The reaction was followed at 390 nm using the bromide salt (10^{-5} M) and a Gilford Automatic Recording Spectrophotometer, model 2400. All solutions were degassed with O_2-free $N_2(Cr^{2+})$ and the cells were capped with teflon caps and sealed with Parafilm. The data was analyzed by the Guggenheim method and exponential fit programs. Generally, the kinetics exhibited first-order decay plots which were

*In ref. 2 an equilibrium constant is given for the protonation as $10^{-8.2}$. The paper does not clearly indicate whether this is K_a or K_b so the measurement has been carried out again and the new values for pK_a are 4.6 (I=0.05 M) and 5.1 (I=0.15 M), at 25 °C [16].

linear over several half-lives. However, some plots exhibited curvature. The latter were ascribed to slow O_2 leakage into the system. Kinetic runs were completed in triplicate and the temperature was controlled with a thermostatted water bath.

Results

Synthesis

The reaction of $(NH_4)_2[OsBr_6]$ with 1,2-ethanediamine results in the synthesis of *cis*-$[Os(en\text{-}H)_2(en)]^{2+}$ (~40–50%) and $[Os(en)_3]^{3+}$ (~40%). At this stage, it is not clear whether $[Os(en)_3]^{3+}$ is produced directly under the reaction conditions or whether the addition of EtOH to precipitate it from the filtrate causes the reduction of the Os^{IV} complex to Os^{III}. In order to maximize these yields, it is necessary to work rapidly, under an O_2-free atmosphere and with anhydrous 1,2-ethanediamine, although reasonable yields can still be obtained without taking these precautions.

The green complex obtained from the filtrate was established as $[Os(en)_3]Br_3$ from its magnetic properties ($\mu_{eff}=1.6$ BM at 20 °C) and its IR and EPR spectra, which were similar to that of $[Os(en)_3]I_3$. This was later confirmed by an X-ray crystallographic analysis of the $[Os(en)_3](CF_3SO_3)_3\cdot H_2O$ salt [7].

Aspects of the structure of the Os^{IV} complex were inferred by the lack of resonances at 7–9 and ~100 ppm in the ^1H and ^{13}C NMR spectra, respectively, typical of imines. In addition, the presence of a single broad ^{13}C NMR signal indicated equivalent carbon atoms on the NMR time scale in water at 32 °C. The broad multiplet in the ^1H NMR spectrum (60 MHz) shows inequivalent en groups which are broadened by exchange. With high field instruments, at low temperature, 5 °C, pH ~7, the amido N-protons were observed as a singlet signal at δ ~13 ppm and the C atom signals were resolved to show the Os^{IV} complex had at least C_2 symmetry in solution [8].

Finally, the definitive characterization was obtained from an X-ray crystallographic analysis (Fig. 1) [6] which showed the molecular ion to be a doubly deprotonated Os^{IV} complex with the deprotonated sites *cis* to each other on separate chelate rings.

The structure of the protonated form of *cis*-$[Os(en\text{-}H)_2(en)]^{2+}$, namely $[Os(en\text{-}H)(en)_2]^{3+}$, was also established by NMR spectroscopy. Initially [3, 6] with the 60 MHz spectrometer at 32 °C in 0.1 M DCl/D_2O only one resonance was observed in the ^{13}C NMR spectrum but with higher field at low temperature and especially in non-aqueous solvents (e.g. CH_3CN) all the C signals were observed [8]. Also, in acetonitrile solution the amido N–H proton was observed as a signal at δ 32 ppm [8]. This complex ion deprotonates reversibly (pK_a ~5) [2, 16] but protonation of the 3^+ cation to $[Os^{IV}(en)_3]^{4+}$ was not detected. No NMR signals were observed for $[Os(en)_3]^{3+}$ under the same conditions.

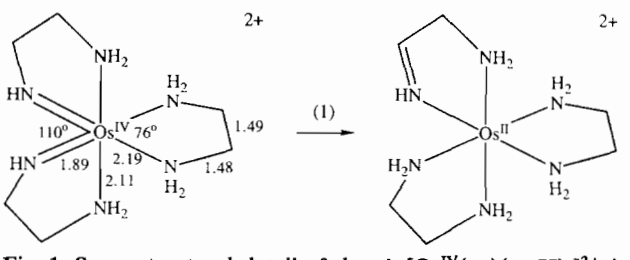

Fig. 1. Some structural detail of the *cis*-$[Os^{IV}(en)(en\text{-}H)_2]^{2+}$ ion [6] and the spontaneous reaction product in the absence of O_2 in aqueous solution.

Solution reactions of the Os^{IV} complexes

When an oxygen-free solution of *cis*-$[Os(en)(en\text{-}H)_2]Br_2$ (10^{-5} M) was allowed to react and the spectra were recorded over a 24 h period, the charge transfer band at 350 nm disappeared and a new one grew at 390 nm, to give a yellow–green solution. Isosbestic points were observed at 318 and 391 nm and the reaction was first-order, ($k_{obs}=\sim 1\times 10^{-5}$ s^{-1}, pH=7.0, $\mu=0.2$ M, 20.4 °C). However, the rate constant varied somewhat in triplicate runs and it is believed that traces of oxygen caused the variation since it was difficult to maintain completely anaerobic conditions over long periods (2 days).

After the solution was exposed to O_2, a third intense charge transfer band grew at 418 nm at the expense of the band at 390 nm. Finally, the charge transfer band grew slowly in intensity and shifted to 423 nm over a period of a week. The various spectral changes are illustrated in Fig. 2.

A similar experiment with *cis*-$[Os(en)(en\text{-}H)_2]I\cdot Br$ was conducted at pH 8.5 (Tris/HCl [17]) at 25 °C. The

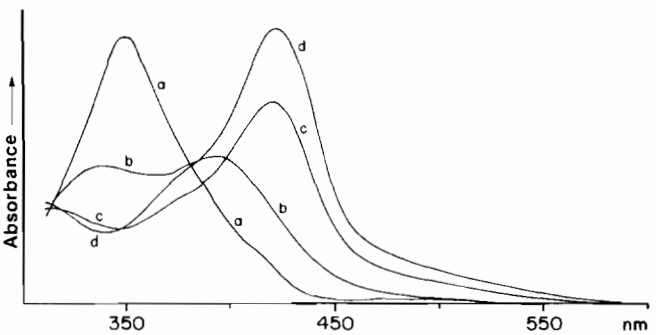

Fig. 2. Spectral changes of *cis*-$[Os(en)(en\text{-}H)_2]Br_2$ (10^{-5} M) in water: a, initial spectrum; b, after 24 h under N_2 atmosphere; c, solution b after 24 h under O_2 (sat.); d, solution c after 1 week in contact with O_2; ϵ_{max} (d) ~14 000 M^{-1} cm^{-1}.

charge transfer bands at 223 and 270 sh were replaced by one at ~400 nm, while the weak band at 550 nm was replaced by one at 680 nm ($\epsilon \sim 100$ M^{-1} cm^{-1}). Isosbestic points were observed at 500 and 330 nm and the spectral changes were much slower than those observed at lower temperatures (20 °C) and pH (7.0). The half-life at pH 8.5 and 25 °C was a matter of days, but it was difficult to follow for such long periods of time because of oxygen sensitivity.

These reactions were also monitored by ^1H and ^{13}C NMR spectroscopy. $[Os(en)(en\text{-}H)_2]Br_2$ was dissolved in O_2-free D_2O, pH 7 and the spectra monitored at intervals over 2 days. The broad pattern at 2.7 ppm (attributed to *cis*-$[Os(en)(en\text{-}H)_2]^{2+}$) decreased and a broad signal at 3.2 ppm grew. Concomitantly signals at 2.5 ppm (methylene) and 7.57 ppm (sharp, singlet CH_2-imine) also grew with time. Exposure of the solution to O_2 caused the new signals to grow and after 4 days the ratio of signals at 2.5, 2.8 and 3.2 was 1:2:1, and the solution was a deep brown–red. Signals due to $[Os^{II}(en)(diim)_2]^{2+}$ were not in evidence.

The reaction was also monitored by ^{13}C NMR spectroscopy. A sample of *cis*-$[Os^{IV}(en)(en\text{-}H)_2]Br_2$ (80 mg) was allowed to react in D_2O (1.5 ml) for 24 h under a N_2 atmosphere, with periodic recording of its ^{13}C NMR spectrum. The initial signal due to *cis*-$[Os^{IV}(en)(en\text{-}H)_2]^{2+}$ disappeared and signals due to $[Os^{II}(en)_2(diim)]^{2+}$ appeared at +94.9 (imine) and −18.1 and −18.3 (en) ppm. Similar observations were made when the complex was exposed to oxygen, or when the triflate salt was used.

In another experiment, a sample of *cis*-$[Os^{IV}(en)(en\text{-}H)_2]I \cdot Br$ (0.2 g) as a suspension in acetone/water (50%, 15 ml) was treated with two equivalents of $AgCF_3SO_3$ [18], whilst the solution was stirred at 0 °C under a blanket of N_2. After 15 min, the mixture was filtered through a bed of Hyflo-Supercel. The residue was washed with O_2-free acetone (2×15 ml) and the combined washings and filtrate freeze-dried at 0.01 torr. This product contained some $[Os^{II}(en)_2(diim)]^{2+}$ (^1H NMR). Similar O_2 oxidation experiments to those described for the bromide salt, resulted in an overall decrease in intensity of all ^1H NMR signals and concomitant broadening of the HDO peak, indicating the presence of paramagnetic species. In addition, the imine peaks became more prominent in comparison to those of the starting material. From these experiments, it was clear that the course of the chemistry was dependent on both the concentrations of the reactant and the nature of the anion.

Solid state reactivity of cis-[Os(en)(en-H)$_2$]Br$_2$

Following ion exchange chromatography of the Os^{IV} complex, the yellow–green leading 2^+ band obtained from the solid state decomposition of the Os^{IV} complex exhibited similar UV–Vis characteristics to that observed in the UV–Vis spectrum of the product of the decomposition of the Os^{IV} complex after one day in deoxygenated water. Other decay products had UV–Vis spectra typical of those observed for $[Os^{II}(en)_2(diim)]^{2+}$ and $[Os^{II}(en)(diim)_2]^{2+}$. When a combined aqueous solution of the first two 2^+ ions that were eluted was maintained in an O_2 atmosphere, the spectrum slowly converted to that expected of the final oxidation product (i.e. $[Os(en)(diim)_2]^{2+}$).

Reactions of [Os(en)$_2$(en-H)]$^{3+}$

$[Os(en)_2(en\text{-}H)]^{3+}$ deprotonates to $[Os(en)(en\text{-}H)_2]^{2+}$ with a pK_a of ~5 [16] but did not protonate to $[Os(en)_3]^{4+}$ even in strong acid, or neat triflic acid, as deduced by UV–Vis spectroscopy.

This complex was relatively stable over a day towards oxidative dehydrogenation in 0.1 M to 1 M HCl, when exposed to the air. However, when reacted with 6 M acid over a 3 day period, $[Os(en)_3]Br_3$ was isolated by the addition of conc. HBr. In addition, the reaction of the Os^{IV} complex with a EtOH/en mixture produced $[Os(en)_3]^{3+}$. The Os^{III} complex was also the product from the $S_2O_4^{2-}$ reduction [1, 2].

Reactions of [Os(en)$_3$]$^{3+}$ and [Ru(en)$_3$]$^{3+}$

When either $[Os(en)_3]^{3+}$ or $[Ru(en)_3]^{3+}$ were allowed to react with OH^- under a N_2 atmosphere, intense charge transfer bands due to imine complexes became evident. In the case of Os^{III}, the spectrum was indicative of the formation of Os^{IV}, prior to the slow generation of the yellow–green solution observed in the decomposition of isolated *cis*-$[Os^{IV}(en)(en\text{-}H)_2]^{2+}$. In the case of Ru, no analogous M^{IV} spectra were observed but only the yellow–green solution with a peak at 375 nm. When the solutions were exposed to air, the more intense charge transfer bands associated with the diimine complexes of Ru^{II} [5] and Os^{II} were apparent.

Similar experiments performed in D_2O/NaOD in air were followed by ^1H NMR spectroscopy. $[Ru^{II}(en)_2(diim)]^{2+}$ formed rapidly in air but $[Os(en)_2(diim)]^{2+}$ formed over about a day (i.e. a similar time-frame to that observed for the oxidation in *cis*-$[Os^{IV}(en)(en\text{-}H)_2]Br_2$).

Electrochemistry

$[Os(en)_3]^{3+}$ showed a reversible reduction to $[Os(en)_3]^{2+}$ at −0.76 V versus SCE in water ($\mu = 0.1$ M, $NaCF_3SO_3$, 20 °C). The one-electron nature of the process was established by coulometry and from the d.c. polarograms using the Heyrovsky–Ilkovic equation. D.c. cyclic voltammograms (Hg) showed a peak to peak separation of 60 mV and i_f/i_r value of 1, showing the reversible one-electron nature of the process. Phase-sensitive a.c. polarograms showed that adsorption pro-

cesses accompanied reduction, since the in-phase component was less that the quadrature component. Comparison of the diffusion current in d.c. polarograms showed that the diffusion coefficient was comparable to that observed for $[Co(en)_3]^{3+}$ under the same conditions.

In dry acetone, both $[Os(en)_3]^{3+}$ and $[Os(NH_3)_6]^{3+}$ displayed reversible reductions to Os^{II} complexes at -0.52 and 0.76 V versus the Ag/AgCl/sat. LiCl(acetone) electrode. Phase-sensitive a.c. polarography showed reversible behaviour up to ~400 Hz. Above this potential, quasi-reversibility was evident; however, the heterogeneous rate constant was too large for an accurate estimate of its value. At very negative potentials (-2.1 V), a second irreversible one-electron reduction was also observed.

Sampled d.c. polarography using a stationary gold working electrode showed what appeared to be a two-electron oxidation of $[Os(en)_3]^{3+}$ at +1.9 V. However, this oxidation process was too close to the solvent oxidation wave to be properly identified.

$[Os(en)(en\text{-}H)_2]^{2+}$ was irreversibly reduced in a two electron process at ~ -1.2 V (versus Ag/AgCl; sat. LiCl) in acetone (Au, Pt or Hg working electrodes). A multielectron oxidation process was apparent also at ~2 V using Au and Pt electrodes. The $[Os(en)_2(en\text{-}H)]^{3+}$ complex was reversibly reduced at +0.29 V under comparable conditions.

EPR spectra and magnetism

Osmium has seven naturally occurring isotopes with ^{187}Os (1.6% natural abundance) and ^{189}Os having nuclear spins of 1/2 and 3/2, respectively [19]. The remaining isotopes apparently have spins of 0, and generally a single broad asymmetric resonance is observed [20], although, a signal due to the ^{189}Os isotope has been resolved at 4 K for $Na_3[OsCl_6]$ [21]. Deviations from octahedral symmetry for Os^{III} complexes cause large variations in g values, generally resulting in three well resolved resonances. The ESR spectrum of $[Os(en)_3]^{3+}$ shows a single broad resonance with g value of 2.15 at -160 °C with a peak-to-peak separation of ~1300 Gauss. The observance of a single peak is consistent with the formulation of an Os^{III} structure with near octahedral symmetry. The magnetic moment of 1.6 BM for $[Os(en)_3]^{3+}$ is close to the spin-only value and in agreement with one unpaired electron. All of this is consistent with the structure of the $[Os(en)_3]^{3+}$ ion in the solid state [6].

UV–Vis spectroscopy

The electronic spectra of the Os^{III} amine complexes were dependent on anions due to outer-sphere charge transfer phenomena. Similar observations have been made previously for $[Ru(en)_3]^{3+}$ [22]. It is more evident in the solid state where $[Os(en)_3]I_3$ is yellow, $[Os(en)_3]Br_3$ is olive-green and $[Os(en)_3](CF_3SO_3)_3$ and $[Os(en)_3]Cl_3$ are colorless. When dissolved in dilute aqueous solution, the coloration decreases for the Br^- and I^- salts, but increases with addition of the respective anion. The electronic spectrum of $[Os^{IV}(en)(en\text{-}H)_2]^{2+}$ is similarly dependent on the anion.

The initial reaction product of the Os^{IV} complex under a N_2 atmosphere gave a yellow–green complex with a charge transfer band at ~400 nm. Also both the Os^{III} and the Os^{IV} complexes reacted with O_2 to form $[Os(en)_2(diim)]^{2+}$ and $[Os(en)(diim)_2]^{2+}$ (Fig. 3), with intense absorptivities at ~410 and 423 nm, respectively. These bands have been attributed to metal→ligand charge transfers, involving transfer of an electron from the filled t_{2g} orbitals of Os^{II} to the π^* orbitals of the imine ligand. Similar charge transfers absorptions are observed for $[Ru^{II}(en)_2(diim)]^{2+}$ [23]. The observation of a charge transfer band at ~400 nm for the intermediate is consistent with the complex containing a monoimine ligand, i.e. $[Os^{II}(en)_2(enim)]^{2+}$. A similar shift to higher energies has been observed in the UV–Vis spectrum of $[Ru^{II}(en)_2(enim)]^{2+}$ (enim = 2-aminoethanimine) in comparison to that of $[Ru^{II}(en)_2(diim)]^{2+}$ [10].

NMR spectroscopy

^1H and ^{13}C NMR spectra were particularly useful for the identification of products containing imine groups. These complexes exhibited sharp resonances in the region of 8–9 ppm in ^1H NMR spectra and at +100 ppm (relative to dioxane) in ^{13}C NMR spectra. The ^{13}C NMR spectrum of $[Os^{II}(en)(diim)_2]^{2+}$ displayed two imine signals (+97.7, +102.8 ppm) due to the imines *cis* and *trans* to 1,2-ethanediamine (-18.6 ppm). The axial and equatorial hydrogen atoms of the 1,2-ethanediamine ligand gave rise to clearly separated signals in the ^1H NMR spectra. This was also particularly marked for the N–H protons where a separation of 2

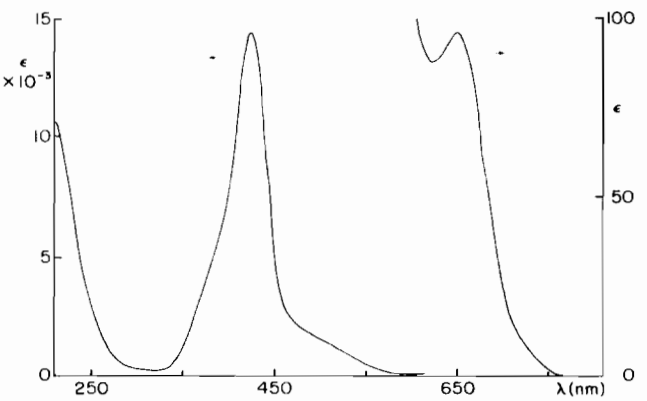

Fig. 3. UV–Vis spectrum of $[Os(en)diim)_2]^{2+}$ in 1 M HCl.

ppm was observed. These large differences in chemical shifts are attributed to a large extension of the filled non-bonding d-orbitals, giving rise to large magnetic anisotropy effects.

The $[Os(en)_2(diim)]^{2+}$ ion possessed a single absorption in its ^{13}C spectrum due to equivalent imine groups (+94.9 ppm). The two sets of inequivalent methylene carbons gave rise to signals at −18.1 and −18.3 ppm. This complex also possessed a characteristically sharp C–^{1}H imine resonance at 7.57 ppm. A ^{1}H NMR imine resonance occurred at 8.50 ppm in the Ru analog [5], and the ^{13}C NMR signals exhibit a similar pattern to those of the Os complex [10].

Discussion

Solution structure of the deprotonated osmium(IV) complexes

The ^{13}C NMR spectra obtained at an operating frequency of 15.09 MHz indicated the equivalence of the ethanediamine rings in both $[Os^{IV}(en)(en\text{-}H)_2]^{2+}$ and $[Os^{IV}(en)_2(en\text{-}H)]^{2+}$. This can only be achieved by rapid proton exchange under these conditions, which makes all the chelates equivalent in a given complex. However, it has been argued previously that the *cis*-$[Os(en)(en\text{-}H)_2]^{2+}$ structure observed in the solid state should also be that which predominates in solution [8]. The broadness of the NMR signal in the ^{1}H NMR spectrum implied that at lower temperatures and/or higher frequencies, this dynamic process could be frozen to reveal the solution structure. In fact the solution structure of *cis*-$[Os(tmen)(tmen\text{-}H)_2]^{2+}$ has been determined by NMR techniques [8], to be essentially the same as that determined for the solid state structure of this complex [8] and for *cis*-$[Os(en)(en\text{-}H)_2]^{2+}$ [6]. Preliminary ^{1}H NMR experiments have been performed on both $[Os^{IV}(en)(en\text{-}H)_2]^{2+}$ and $[Os^{IV}(en)_2(en\text{-}H)]^{2+}$ at 400 MHz in both aqueous and acetonitrile solutions*. These experiments show that the structures observed in the solid state are maintained in solution. Moreover, deuteration was not instantaneous, as initially reported [25], but the NH protons were observed in D_2O when solutions of either complex were prepared at ~5 °C and the spectra recorded rapidly [24]. The details of the solution structure, and the dynamics and mechanism of the proton exchange rate will be discussed elsewhere, but a salient point in the discussion of the mechanisms that follow is that the solid state structure is relevant to possible mechanistic schemes.

*There is exchange of protons in aqueous solution on the timescale of minutes, so that the NH protons are not observed unless spectra are recorded rapidly and at low temperatures. However, in acetonitrile, proton transfer is slow and the complex exhibits the same structure as observed in the solid state [24].

Mechanisms of oxidative dehydrogenation reactions

Although there have been extensive studies into the mechanisms of oxidative dehydrogenation reactions of amine ligands coordinated to iron [10, 26–32] and ruthenium [5, 9, 23, 33–36], this was the first example of similar chemistry being observed at Os^{IV} [3, 6, 37]. It was also the first time that it was established that the M^{IV} oxidation state was an intermediate in the oxidative dehydrogenation reactions (at least for Os) [3, 6, 37]. This result is germane to the development of a more general mechanistic scheme for the oxidative dehydrogenation reactions of amine and alcohol complexes of the Fe group, which involves spontaneous oxidative dehydrogenation reactions of M^{IV} complexes that were generated from base-catalyzed disproportionation of the M^{III} species [3, 6, 37]. The characterization of these Os^{IV} species assisted in the development of the detailed mechanistic schemes for the oxidation of amine complexes [3, 6, 33, 34].

Despite the unequivocal evidence that the osmium chemistry presents for the involvement of the M^{IV} oxidation state in such mechanistics schemes, the original mechanisms [29, 30], that are based on the formation of radical cation complexes of M^{III} as the reactive intermediates, still persist [27, 28, 31, 32]. Therefore, it is pertinent to discuss details of the osmium chemistry in the context of more recent work on Fe and Ru complexes [9, 10], that impinges on the mechanism.

cis-$[Os(en(en\text{-}H)_2]^{2+}$ has been shown to undergo spontaneous decomposition in deoxygenated aqueous solution to give a yellow–green mono-imine complex (absorption ~390–400 nm). Its general chemistry is consistent with analogous Ru chemistry, where the product of the spontaneous decomposition of the Ru^{IV} complexes has been shown to be $[Ru(en)_2(enim)]^{2+}$ [10]. Therefore, the decomposition of the Os^{IV} complex in dilute (10^{-5} M) solutions, or in the solid state is an intramolecular $2e^-$ oxidation of the ligand by Os^{IV} (Fig. 1, reaction (1)).

cis-$[Os(en)(en\text{-}H)_2]^{2+}$ is readily protonated to form $[Os(en)_2(en\text{-}H)]^{3+}$ (pK_a 5 [2, 16]), which has been established to be a much stronger oxidant than the 2^+ ion from the electrochemical experiments (>1 V). Therefore, the rate of intramolecular oxidation is expected and qualitatively observed to be faster at lower pH. This is consistent with recent chemistry of Fe and Ru amine complexes, where the monodeprotonated M^{IV} complexes undergo much more rapid spontaneous intramolecular oxidations than the doubly-deprotonated analogues [9, 10]. At very low pH values, it seems that the oxidizing power of the Os^{IV} complex is such that intramolecular oxidative dehydrogenation reactions via disproportionation are no longer competitive with intermolecular oxidation of halide ion and/or water and the preferred reduction product is $[Os(en)_3]^{3+}$. How-

ever, another possible implication of this result is that the $[Os(en)_3]^{4+}$ ion is being produced in low concentrations and its redox potential ($\geqslant 2$ V) is sufficient to oxidize the halide ion or water rapidly by outer sphere electron transfers, even though its concentration is necessarily small. This complication is not as evident in analogous Fe^{IV} and Ru^{IV} chemistry, where the spontaneous intramolecular oxidative dehydrogenation reactions are many orders of magnitude faster than for Os^{IV} [9, 10].

There appear to be at least three possible mechanisms for reaction (1) (Scheme 1). The first is a tautomerization-like reaction akin to those observed in the acid-catalyzed enol formation from aldehydes and ketones, or enamines from imines, reaction (2). The second, reaction (3), is an intramolecular hydride transfer from a methylene group to an imide nitrogen on the adjacent chelate (3). The third, reaction (4), is the transfer of a hydride ion to Os^{IV} as the first step [34, 9].

Of these three possible mechanisms, the evidence to date favours that depicted in reaction (2). $[Os(en)_2(en\text{-}H)]^{3+}$, for example, is a much better oxidant that $[Os(en)(en\text{-}H)_2]^{2+}$. The 3+ ion is also more acidic than the 2+ ion. Both factors would lead to an increase in rate for the mechanism in reaction (2). The first, by simple application of Marcus–Hush theories of intramolecular electron transfer [38–41]. The second, by a faster proton loss. The mechanism in reaction (3), however, would not be feasible for the 3+ ion since two Os=N moieties are required and it can therefore be eliminated. The hydride transfer in reaction (4) is semi-consistent with the data. The high redox potential of the 3+ ion would enhance hydride abstraction but the increase in acidity is not necessarily consistent with the rate increase.

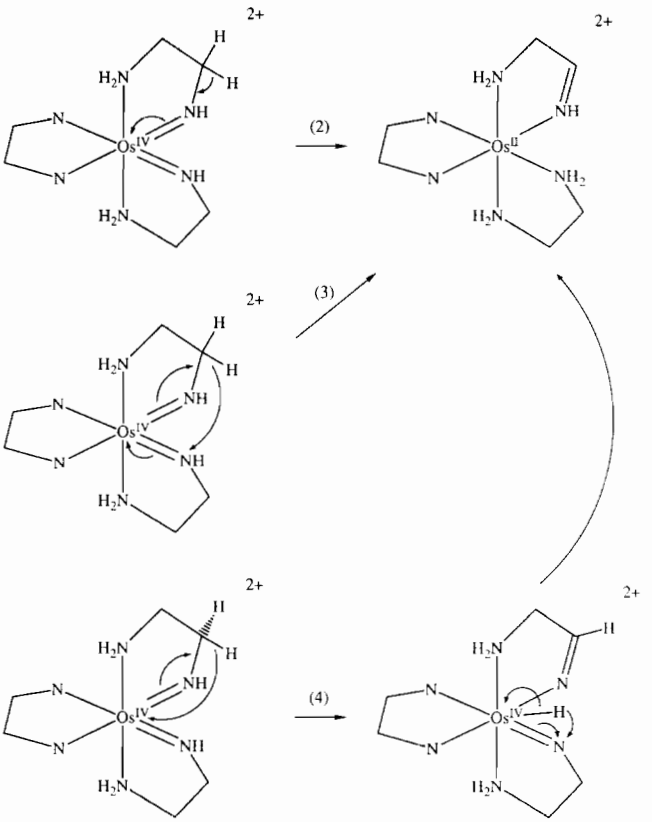

Scheme 1. Mechanistic paths for the redox reaction of $[Os^{IV}(en)(en\text{-}H^+)_2]^{2+}$.

Detailed kinetic analyses in Ru complexes [9, 10] show that analogous oxidations occur with rate constants about five orders of magnitude larger than those for Os. Since the $[Ru(en)_3]^{3+/2+}$ couple [42] is ~ 0.7 V more positive than that observed for the $[Os(en)_3]^{3+/2+}$ couple, it is also expected that Ru^{IV} complexes will be stronger oxidants than their Os^{IV} analogues. This effect favors both mechanisms (2) and (4). The π-bonding stabilization of the M^{IV} species by deprotonated amines is greater for Os than Ru simply because of the greater radial extension of its d orbitals. This is displayed in the K_a values of $[M(en)_2(en\text{-}H)]^{3+}$ which differ by $\sim 10^3$ with Os more acidic than Ru [10]. The effect is also seen in the ability of Ru^{III} and Os^{III} to undergo π-bonding with the Cl^- ion [43]. While the higher Ru redox potential is consistent with the more rapid hydride transfer, it would be expected that Os would stabilize the hydride more effectively. Finally, there is indirect evidence in the $[Ru^{IV}(sar\text{-}2H^+)]^{2+}$ amine oxidation [9] of a general base path, presumably abstraction of the proton in reaction (2) to trigger the redox cascade to imine and Ru^{II}. On balance therefore, it seems that the mechanism depicted in reaction (2) is the most likely.

The analogy between reaction (2) and the acid-catalyzed enolization of aldehydes and ketones is valid. In the organic chemistry the protonated oxygen causes β-elimination of a proton to form the enol (eqn. (5)). The osmium chemistry can be viewed similarly (eqn. (6)).

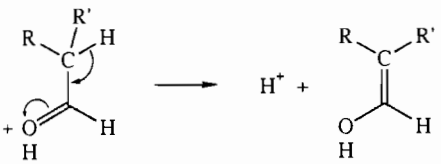

(5)

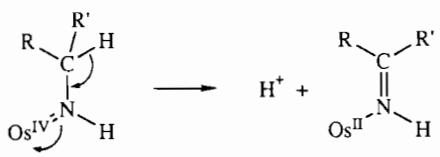

(6)

When one amide of the Os^{IV} complex is protonated, the Os^{IV} center becomes more electron deficient and therefore reaction (6) proceeds more rapidly. There is

^{1}H NMR spectroscopic evidence in solution that the Os^{IV} ground state can be viewed in the manner depicted. The α-proton attached to the carbon of imines and aldehydes has a chemical shift that typically occurs at 8–10 ppm downfield from TMS, and this resonance is expected to move further downfield on protonation of the heteroatom of the double bond. Therefore, if the Os^{IV}=NHR moiety can be viewed as an aldehyde or imine equivalent, a downfield chemical shift is expected for the proton on the Os=NH double bond. This is indeed the case and the downfield chemical shift is found to be 13 ppm for both $[Os(en)(en\text{-}H)_2]^{2+}$ [24] and the related complex, $[Os(tmen)(tmen\text{-}H)_2]^{2+}$ [8]. This resonance shifts to 32 ppm for $[Os(en)_2(en\text{-}H)]^{3+}$ [24] and 30 ppm for $[Os(tmen)_2(tmen\text{-}H)]^{3+}$ [8] indicating a further polarization of the bonding, consistent with the mono-deprotonated species being more activated. The imine or aldehyde-type character of the Os^{IV}=N bonds is also evident in the X-ray structures of $[Os(en)(en\text{-}H)_2]^{2+}$ [6] and $[Os(tmen)(tmen\text{-}H)_2]^{2+}$ [8] and related molecules [34, 35] where it is clearly shown that Os–N, Ru–N multiple bonds are present. Also, the sp^2 hybridization about the N of the Os=N and Ru=N double bonds was established in the structures.

Some comment needs to be made about why reaction (1) (Fig. 1) is not seen at the higher concentrations of Os^{IV} that are used in NMR experiments. Rather, $[Os(en)_2(diim)]^{2+}$ appears to be the major oxidation product, from both ^{1}H and ^{13}C NMR spectroscopy experiments. In Ru and Fe oxidations, this is generally not the case, since the mono-imine complexes can usually be observed and characterized [9, 10]. In the osmium chemistry, the formation of $[Os(en)_2(diim)]^{2+}$ directly from $[Os(en)(en\text{-}H)_2]^{2+}$ can be explained by the reactions shown in Scheme 2*. Rapid disproportionation of the Os^{III} imine complex is also a likely path. For example, $[Ru^{III}(trpy)(bpy)(HN{=}CR_2)]^{3+}$ complexes disproportionate extremely rapidly to Ru^{II} and Ru^{IV}, as evidenced by the net $2e^-$ oxidation of the Ru^{II} analogue to the deprotonated Ru^{IV} complex $[Ru^{IV}(tripy)(bpy)(N{=}CR_2)]^{3+}$, even under acidic conditions [35]. Such intermolecular reactions could occur readily in high concentrations of Os^{IV}, where the second-order oxidation to the product by Os^{IV} becomes competitive with the first-order intramolecular electron transfer in $[Os^{IV}(en)(en\text{-}H)_2]^{2+}$ ($t_{1/2}$ = 19 h, 25 °C, pH = 7.0) to produce $[Os^{II}(en)_2(enim)]^{2+}$. Once formed, the methylene group adjacent to the imine of $[Os^{IV}(en)_2(enim\text{-}2H)]^{2+}$, is expected to be even more activated than those of $[Os^{IV}(en)(en\text{-}H)_2]^{2+}$, thus leading to the preferred product, $[Os(en)_2(diim)]^{2+}$, even though the Os^{IV}(enim) complex should be an inferior oxidant.

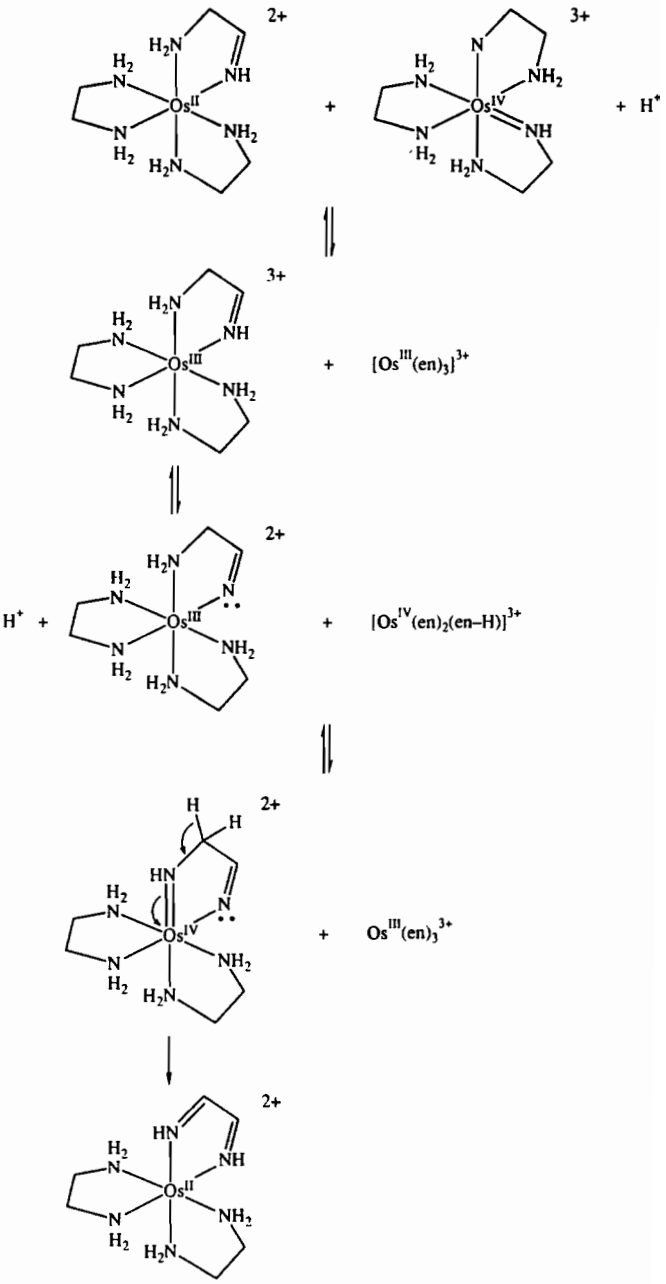

Scheme 2. Proposed mechanistic path for the generation of $[Os^{II}(en)_2(diim)]^{2+}$.

The reason for the absence of the direct formation of diimine species from Ru^{IV} and Fe^{IV} amine complexes in their spontaneous oxidative dehydrogenation reactions, probably arises from the more rapid intramolecular oxidations. There rate constants are typically five orders of magnitude greater [9, 10] than those observed in the osmium chemistry, and hence, the second-order oxidations of the M^{II}–mono-imine com-

*There are also other redox reactions that could produce $[Os^{IV}(en)_2(enim\text{-}2H)]^{2+}$, and a variety of isomers of the deprotonated species, but these have not been included for simplicity.

plexes by M^{IV} are not competitive with the first-order oxidative dehydrogenation reactions. However, diimine complexes are formed as primary products in the base-catalyzed decomposition of $[Fe(CN)_4(diamine)]^-$ complexes [26–28, 31].

Mechanisms of oxidative dehydrogenation reactions of M^{II} and M^{III} amine complexes

The redox reactions of $[M(en)_3]^{3+/2+}$ in water indicate that one of the products is the $[M^{II}(en)_2(enim)]^{2+}$ complex*. This could arise from the disproportionation of $[M^{III}(en)_3]^{3+}$ to form $[M^{II}(en)_3]^{2+}$ and $[M^{IV}(en)(en\text{-}H)_2]^{2+}$ or $[M^{IV}(en)_2(en\text{-}H)]^{3+}$, depending on the pH. The oxidative dehydrogenation reaction would then proceed as before. This is indirect evidence for the involvement of the M^{IV} oxidation state in the decomposition of M^{III} complexes of the iron group.

In the case of $[Os^{III}(en)_3]^{3+}$, it is clear that one of the initial products of the reaction of the complex in base under N_2 is $[Os^{IV}(en)(en\text{-}H)_2]^{2+}$, which only reacts slowly to produce $[Os^{II}(en)_2(enim)]^{2+}$. No intermediates were observed initially in the Ru chemistry, where the product first observed was $[Ru(en)_2(enim)]^{2+}$. However, on the shorter time scale available with stopped-flow techniques, it has now been established that this type of reaction proceeds via an initial disproportionation of the Ru^{III} complex to Ru^{IV} and Ru^{II} [10].

The chemistry of $[Os(en)_3]^{3+}$ enables the mechanism of the initial disproportionation reaction to be determined. Since $[Os(en)_3]^{4+}$ cannot be observed directly even by protonation of $[Os(en)_2(en\text{-}H)]^{3+}$ in strong acid, then an initial disproportionation of the type shown in reactions (7) and (8) can be excluded.

$$2[Os(en)_3]^{3+} \rightleftharpoons [Os(en)_3]^{2+} + [Os(en)_3]^{4+} \quad (7)$$

$$[Os(en)_3]^{4+} \rightleftharpoons [Os(en)_2(en\text{-}H)]^{3+} + H^+ \quad (8)$$

The negative redox potential of the $Os^{III/II}$ couple (-0.52 versus NHE) and the very positive potential of the $Os^{IV/III}$ couple ($\gtrsim 2$ V) means that the forward rate must be extremely slow and the back reaction close to diffusion controlled. Also, the rate constant for the reaction of Ru^{III} would be far too slow to be the first step in the rapid base-catalyzed oxidative dehydrogenation reactions of $[Ru(en)_3]^{3+}$. Therefore, the initial step in the oxidative dehydrogenations that is consistent with all the results is a mechanism that involves initial deprotonation of $[M(en)_3]^{3+}$ (eqns. (9)–(11)).

*This has been substantiated in the case of $[Ru(en)_3]^{3+}$, where detailed kinetics have also supported the mechanism proposed. Moreover, the deprotonated $[Ru^{III}(en)_2(en\text{-}H)]^{2+}$, $[Ru^{IV}(en)_2(en\text{-}H)]^{3+}$ and $[Ru^{IV}(en)(en\text{-}H)_2]^{2+}$ intermediates have been characterized [10].

$$[M(en)_3]^{3+} + OH^- \rightleftharpoons [M(en)_2(en\text{-}H)]^{2+} + H_2O \quad (9)$$

$$[M(en)_3]^{3+} + [M(en)_2(en\text{-}H)]^{2+} \rightleftharpoons [M(en)_3]^{2+} + [M(en))_2(en\text{-}H)]^{3+} \quad (10)$$

$$[M(en)_2(en\text{-}H)]^{3+} + OH^- \rightleftharpoons \downarrow -H^+$$

$$[M(en)(en\text{-}H)_2]^{2+} \longrightarrow M(en)_2(enim)^{2+} \quad (11)$$

While the work presented here does not enable us to distinguish between all possibilities, stopped-flow experiments have enabled the characterization of a number of Fe^{III} and Ru^{III} deprotonated complexes, that then undergo disproportionation [9, 10]. This is consistent with the overall chemistry outlined in Scheme 3 for the redox chemistry of the osmium/1,2-ethanediamine system**.

It is clear now, that all spontaneous reactions of Fe [10], Ru [9, 10] and Os amine complexes that produce imines, which have been studied in sufficient depth, appear to proceed via M^{IV} intermediates. There is no direct evidence, to our knowledge, in support of M^{III}–amine radical cations invoked [25–28] as reactive intermediates in these systems. The role of ligand deprotonation/protonation equilibria to initiate these reactions is very important and its role is two-fold. It enables the stabilization of the high formal oxidation states by strong π-bonding, thereby driving the disproportionation. The M^{IV} oxidation state also activates the ligand towards oxidation via a tautomerization type mechanism, in much the same way that multiple bonding and attachment of an electron withdrawing group, activates the formation of enols and enamines, in aldehydes and imines, respectively.

The results and arguments presented here provide convincing evidence for the general involvement of M^{IV}

**It has been argued by Bernhard and Anson [36] that the disproportionation of $[Os(en)_3]^{3+}$ to $[Os(en)_3]^{2+}$ and $[Os(en)_2(en\text{-}H)]^{3+}$ is highly unfavourable thermodynamically, which was obvious from our previously published electrochemical data [6]. They indicated that our observed disproportionation was due to the formation of $[Os(en)(en\text{-}H)_2]^{2+}$, or O_2 contamination which oxidized Os^{II}, and thereby driving the equilibrium. The answer to their apparent dilemma was already contained in our original communication, where we indicated that $[Os(en)(en\text{-}H)_2]^{2+}$ was irreversibly reduced in a two-electron step to Os^{II}. For this to occur, it is necessary that deprotonated $[Os(en)_3]^{3+}$ complexes must rapidly disproportionate in solution. Under the basic conditions used to follow the decomposition of $[Os(en)_3]^{3+}$, $[Os(en)(en\text{-}H)_2]^{2+}$ is the thermodynamically stable form of Os^{IV}. Therefore, the electrochemical results presented previously [6] and pK_a information of the Os^{IV} complexes [2, 16] establishes that such a disproportionation is highly favoured thermodynamically. It is also observed to occur very rapidly.

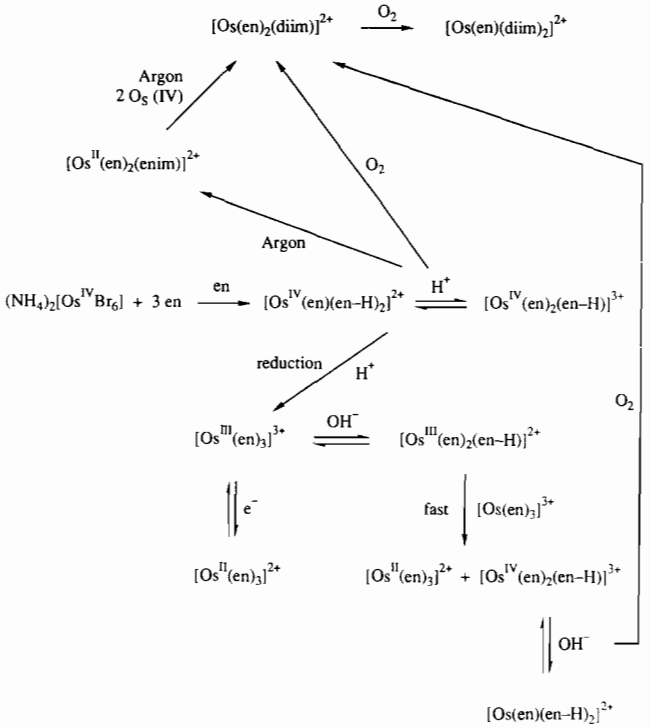

Scheme 3. Redox reactions of osmium ethanediamine and imine complexes.

oxidation states in the oxidative dehydrogenation reactions of amine complexes of the Fe group. Not only has the Os chemistry been extremely useful in helping elucidate the mechanisms of such reactions, but it has also been useful synthetically. For instance, similar chemistry has been used to prepare $[(NH_3)_5OsNCCNOs(NH_3)_5]^{n+}$ complexes from $[(NH_3)_5Os(NH_2CH_2CH_2NH_2)Os(NH_3)_5]^{6+}$ [44]. This is an important path since NCCN is too poor a donor and too readily hydrolyzed when bound to Os^{III} to prepare the complex from $[Os^{III}(NH_3)_5(OSO_2CF_3)]^{2+}$, and the ligand is too readily reduced to use Os^{II} species in its preparation. It is also likely that the type of chemistry outlined will have other applications in the preparation of complexes that are difficult to access by other routes.

Acknowledgements

We are grateful to the microanalytical services of the Research School of Chemistry, A.N.U. and for helpful discussions on the related tmen chemistry and the NMR of the Os^{IV}–en complexes with A. Patel, H.-B. Bürgi and A. Ludi.

References

1 F. P. Dwyer and J. W. Hogarth, *J. Am. Chem. Soc., 75* (1953) 1008.
2 F. P. Dwyer and J. W. Hogarth, *J. Am. Chem. Soc., 77* (1955) 6152.
3 P. A. Lay, *Ph.D. Thesis,* Australian National University, 1981, Ch. 6.
4 H. Elsbernd and J. K. Beattie, *J. Chem. Soc. A,* (1970) 2598.
5 B. C. Lane, J. E. Lester and F. Basolo, *J. Chem. Soc., Chem. Commun.,* (1971) 1618.
6 P. A. Lay, A. M. Sargeson, B. W. Skelton and A. H. White, *J. Am. Chem. Soc., 104* (1982) 6161.
7 P. A. Lay, G. McLaughlin and A. M. Sargeson, *Aust. J. Chem., 40* (1987) 1267.
8 A. Patel, A. Ludi, H.-B. Bürgi, A. Raselli and P. Bigler, *Inorg. Chem.,* in press.
9 P. Bernhard and A. M. Sargeson, *J. Am. Chem. Soc., 111* (1989) 597.
10 D. J. Bull, *Ph.D. Thesis,* Australian National University, 1991.
11 S. Brownstein, J. Bornais and G. Latremouille, *Can. J. Chem., 56* (1978) 1419.
12 F. P. Dwyer and J. W. Hogarth, *Inorg. Synth., 5* (1957) 204.
13 I. P. Evans, G. W. Everett and A. M. Sargeson, *J. Am. Chem. Soc., 98* (1976) 8041.
14 J. W. Hogarth and F. P. Dwyer, *J. Proc. R. Soc. N.S.W., 85* (1951) 113.
15 B. W. Skelton and A. H. White, unpublished results, 1977.
16 A. Patel, unpublished results.
17 D. D. Perrin, *Aust. J. Chem., 16* (1963) 572.
18 W. G. Jackson, G. A. Lawrance, P. A. Lay and A. M. Sargeson, *Aust. J. Chem., 35* (1982) 1561.
19 R. C. Weast, *CRC Handbook of Chemistry and Physics,* The Chemical Rubber Company, Florida, 58th edn., 1978, Sect. B.
20 R. S. Abdrakhmanov, N. S. Garif'yanov and E. I. Semenova, *Russ. J. Inorg. Chem., 17* (1972) 613.
21 A. Aràneo, G. Mercati, F. Morazzoni and I. Napoletano, *Inorg. Chem., 16* (1977) 1196.
22 H. Elsbernd and J. K. Beattie, *Inorg. Chem., 7* (1968) 2468.
23 D. F. Mahoney and J. K. Beattie, *Inorg. Chem., 12* (1973) 2561.
24 P. A. Lay and A. Patel, unpublished results.
25 J. W. Palmer and F. Basolo, *J. Inorg. Nucl. Chem., 15* (1960) 279.
26 V. L. Goedken, *J. Chem. Soc., Chem. Commun.,* (1972) 207.
27 M. Goto, M. Takeshita, N. Kanda, T. Sakai and V. L. Goedken, *Inorg. Chem., 24* (1985) 582.
28 Y. Kuroda, N. Tanaka, M. Goto and T. Sakai, *Inorg. Chem., 28* (1989) 2163.
29 V. L. Goedken and D. H. Busch, *J. Am. Chem. Soc., 94* (1972) 7355.
30 J. C. Dabrowiak, F. V. Lovecchio, V. L. Goedken and D. H. Busch, *J. Am. Chem. Soc., 94* (1972) 5502.
31 A. M. da Costa Ferreira and H. E. Toma, *J. Chem. Soc., Dalton Trans.,* (1983) 2051.
32 H. E. Toma, A. M. da Costa Ferreira and N. Y. Murakami Iha, *Nouv. J. Chim., 9* (1985) 473.
33 M. J. Ridd and F. R. Keene, *J. Am. Chem. Soc., 103* (1981) 5733.
34 F. R. Keene, M. J. Ridd and M. R. Snow, *J. Am. Chem. Soc., 105* (1983) 7075.
35 P. A. Adcock, F. R. Keene, R. S. Smythe and M. R. Snow, *Inorg. Chem., 23* (1984) 2336.
36 P. Bernhard and F. C. Anson, *Inorg. Chem., 28* (1989) 3272.

37 P. A. Lay, A. M. Sargeson and A. H. White, *COMO-9 Abstracts,* Royal Australian Chemical Institute, Sydney, 1990, p. 32.
38 N. S. Hush, *NATO Adv. Study Inst. Ser., Ser. C, 58* (1980) 151.
39 R. A. Marcus, *Ann. Rev. Phys. Chem., 72* (1968) 155.
40 R. A. Marcus, *J. Phys. Chem., 72* (1968) 891.
41 W. J. Albery, *Ann. Rev. Phys. Chem., 31* (1980) 227.
42 T. J. Meyer and H. Taube, *Inorg. Chem., 7* (1968) 2369.
43 T. W. Hambley and P. A. Lay, *Inorg. Chem., 25* (1986) 4553.
44 P. A. Lay and H. Taube, to be published.